International Journal for Multiscale Computational Engineering, 8(3), 331–342 (2010)

CONTINUUM AND ATOMISTIC MODELING OF THE MIXED STRAIGHT DISLOCATION

Paweł Dłużewski,[1,*] Toby D. Young,[1] George P. Dimitrakopulos,[2] & Philomela Komninou[2]

[1]*Institute of Fundamental Technological Research, Polish Academy of Sciences, ul. Pawińskiego 5 B, 02-106 Warsaw, Poland*

[2]*Department of Physics, Aristotle University of Thessaloniki, GR-54124 Thessaloniki, Greece*

[*]Address all correspondence to Paweł Dłużewski E-mail: pdluzew@ippt.gov.pl

A continuum and atomistic approach to the modeling of dislocations observed by high-resolution transmission electron microscopy (HRTEM) is discussed in terms of the continuum theory of dislocations. The atomistic models are obtained by means of the use of a mathematical formula for discrete dislocations. A new analytical solution for a continuously distributed dislocation core is presented. This solution is employed in the finite element modeling of residual stresses induced by the net of dislocations visible on an HRTEM image of GaN structure. This paper terminates with some comments on the atomistic/finite-element modeling of dislocation fields. Because of some confusion concerning notations used in the literature, the mathematical foundations of the continuum theory of dislocations are revisited.

KEY WORDS: *dislocations, field theory, atomistic models, finite element method, high-resolution transmission electron microscopy*

1. INTRODUCTION

In the continuum theory of dislocations the antisymmetric parts of tensor gradients take on an important role. In tensor calculus a few different methods of tensor differentiation are used. In result, some differential operators written according to different conventions can take a different sign. At the origin of dislocation theory the classical convention was often based on the left-hand covariant differentiation of tensors (see Kröner, 1958; de Wit, 1960, 1970; Teodosiu, 1970). It was closely related to the use of the nabla operator, rewritten usually on the left-hand side of tensors (see Table 1). Recently, in the finite deformation approach based on the multiplicative (polar) decomposition of the displacement deformation gradient the right-hand differentiation has become the main convention. This convention is based on the use of a comma as a separator between the subscripts and components of covariant derivatives of a tensor.

Unfortunately, over many years, in the continuum theory of dislocations the finite deformations were identified with a very specific approach based on the use of a convex coordinate system related to the deformation of crystal lattice. In this approach, due to incompatibilities induced by dislocations, the coordinate system leaves a three-dimensional (3D) Euclidean space and, together with the metric tensor generated by the scalar product of the crystal lattice vectors, composes a 3D Riemannian space on which the teleparallel connection generated by the lattice vector differentiation can be determined [see Kondo (1952, 1963), Bilby (1960), Gairola (1979)].

Another approach to finite deformation, based on the use of the standard (immobile) coordinate systems, Eulerian and Lagrangian, was developed. In this case the geometry and deformation are considered in the Lagrangian (reference) and Eulerian (actual, deformed) configurations, respectively. Such an approach is employed in the present paper. To admit the initial lattice incompatibilities in the reference configuration an additional local configuration has been introduced by Teodosiu (1970). He called it a *local isoclinic relaxed configuration*. Recently, the configuration has often been called the intermediate con-

1543–1649/10/$35.00

TABLE 1: Differential operators and fundamental tensors of dislocation theory rewritten in different conventions.

	Differentiation based on nabla convention		Vs.	Right–hand covariant differentiation
	Tensor notation	Index notation	Transition	Index notation
$\operatorname{grad}\mathbf{t}$	$\nabla\mathbf{t}$	$\nabla_i t_{j_1\cdots j_n}$	$\operatorname{grad}\mathbf{t} \Rightarrow \operatorname{grad}^T\mathbf{t}$	$t_{i_1\cdots i_n,j}$
e.g.,		$\beta_{ij} \stackrel{\text{df}}{=} \nabla_i u_j$	$\boldsymbol{\beta} \Rightarrow \boldsymbol{\beta}^T$	$\beta_{ij} \stackrel{\text{df}}{=} u_{i,j}$
$\operatorname{curl}\mathbf{t}$	$\nabla\times\mathbf{t}$	$e_{ikj_1}\nabla_k t_{j_1\cdots j_n}$	$\operatorname{curl}\mathbf{t} \Rightarrow -\operatorname{curl}^T\mathbf{t}$	$t_{i_1\cdots i_n,k}\, e_{ji_nk}$
e.g.,		$\alpha_{ij} \stackrel{\text{df}}{=} -e_{ikl}\nabla_k\beta_{lj}$	$\boldsymbol{\alpha} \Rightarrow \boldsymbol{\alpha}^T$	$\alpha_{ij} \stackrel{\text{df}}{=} \beta_{ik,l}\, e_{jkl}$
		$b_i = \int \alpha_{ji}\, ds_j$	$\mathbf{b} \Rightarrow \mathbf{b}$	$b_i = \int \alpha_{ij}\, ds_j$
		$l_i\, b_j = \int \alpha_{ij}\, dv$	$\mathbf{l} \Rightarrow -\mathbf{l}$	$b_i\, l_j = \int \alpha_{ij}\, dv$
$\operatorname{inc}\mathbf{t}$	$\nabla\times\mathbf{t}\times\nabla$	$e_{ikl_1}\nabla_k t_{l_1l_2}\nabla_m\, e_{jl_2m}$	$\operatorname{inc}\mathbf{t} = -\operatorname{inc}^T\mathbf{t}$	$t_{j_1\cdots j_n,k_1\cdots k_n} e_{i_1j_1k_1}\cdots e_{i_nj_nk_n}$
e.g.,		$\eta_{ij} \stackrel{\text{df}}{=} e_{ikl}\nabla_k\beta_{lm}\nabla_n\, e_{jmn}$	$\boldsymbol{\eta} \Rightarrow \boldsymbol{\eta}^T$	$\eta_{ij} \stackrel{\text{df}}{=} -\beta_{kl,mn}\, e_{ikm}\, e_{jln}$

figuration. Contrary to the previous concept proposed by Kondo and Bilby, in this case the local coordinate system is used only for local manipulation of tensors in the so-called tangent vector space, while all consideration on the topology of crystal lattice is considered in a 3D-oriented Euclidean space. As outlined above, in tensor calculus two different conventions of the right- and left-hand covariant differentiations are used, resulting in a transposition and a different sign obtained for the representation of some tensors. The most important differences for the dislocation theory have been gathered in Table 1. In order to limit discussion on various tensor representations and focus our attention on computational aspects, we focus our interest on the description of dislocation tensor fields in the orthonormal coordinate systems in a 3D Euclidean space.

In the present paper the right-hand covariant differentiation is used, and the Stokes theorem takes the form

$$\oint_o \mathbf{t}\, d\mathbf{x} = -\int_s \operatorname{curl}\mathbf{t}\, d\mathbf{s}, \tag{1}$$

where $d\mathbf{s}$ denotes a surface element vector, the sense of which is generated by the clockwise circulation according to the right-hand rule (cf. Table 1). For comparison, the traditional notation based on the nabla convention leads to a positive sign on the right side of the last equation.

The paper is organized as follows: In Section 2 the mathematical foundations of the continuum theory of dislocations are revisited in the convention based on the right-hand covariant differentiation. In Section 3 a new analytical solution for distribution of the dislocation core is presented; this is followed by a short discussion of the classical formula for discrete dislocations. In Section 4 a numerical example of the finite element modeling of dislocations and residual stresses is discussed. The example concerns dislocations visible on the high-resolution transmission electron microscopy (HRTEM) image of a GaN sample. The nonlinear finite element approach is based on the anisotropic hyperelastic elements. The paper ends with some comments on the role of the orientation field in computer modeling and preprocessing the atomistic and continuous models of dislocations.

2. CONTINUUM THEORY OF DISLOCATIONS

In the linear theory of dislocations the gradient of crystal deformation is decomposed additively into the lattice and plastic distortion tensors according to

$$\operatorname{grad}\mathbf{u}_{\text{tot}} = \boldsymbol{\beta} + \boldsymbol{\beta}_{\text{pl}} \tag{2}$$

[cf. Kröner (1981)]. By assumption, the lattice distortion $\boldsymbol{\beta}$ is composed of the antisymmetric tensor of crystal lattice rotation, $\mathbf{w} = -\mathbf{w}^T$, and the symmetric tensor of elastic strain $\boldsymbol{\varepsilon} = \boldsymbol{\varepsilon}^T$,

$$\boldsymbol{\beta} = \mathbf{w} + \boldsymbol{\varepsilon}. \tag{3}$$

The plastic distortion $\boldsymbol{\beta}_{\text{pl}}$ is identified with an asymmetric strain tensor being isoclinic with the lattice rotation. This nomenclature comes from the theory of elasto-plastic Cosserat continua where the particle rotation $\boldsymbol{\chi}$ and elastic/plastic strains are identified by $\boldsymbol{\chi} \equiv \mathbf{w}$, $\boldsymbol{\varepsilon} \equiv \boldsymbol{\varepsilon}$, and $\boldsymbol{\varepsilon}_{\text{pl}} \equiv \boldsymbol{\beta}_{\text{pl}}$ respectively, which gives

$$\operatorname{grad}\mathbf{u}_{\text{tot}} = \boldsymbol{\chi} + \boldsymbol{\varepsilon} + \boldsymbol{\varepsilon}_{\text{pl}}, \tag{4}$$

where $\boldsymbol{\epsilon}$ is no longer symmetric. Contrary to the Cosserat continua, in the continuum theory of dislocations it is assumed that the particle cannot rotate independently of the displacement field and therefore, a simplified notation combining the elastic strain and crystal lattice rotation into a common lattice distortion tensor $\boldsymbol{\beta}$ became more convenient.

2.1 Burgers Vector

The sense of the Burgers vector depends on the assumed sense of dislocation line, as well as on the convention used to determine the Burgers circuit. Our intention is that the definitions used in this paper are to be in agreement with those used in crystallography and in the textbook by Hirth and Lothe (1982) devoted to the mathematical theory of discrete dislocations. The orientation of the edge dislocation vs. coordinate system assumed here is shown in Fig. 1. According to this convention, the sense of the Burgers vector coincides with the sense of the x axis, while the sense of a dislocation line corresponds to dislocation piercing the paper out to the sheet [cf. Figs. 3–10 in Hirth and Lothe (1982)]. Obviously, if the dislocation line is oriented into paper, then according to this convention, the resultant sense of the Burgers vector is opposite [cf. Figs. 1–21 and 1–22 in the textbook mentioned].

Before limiting our interest to the linear theory (infinitesimal strain approach) it is convenient to consider the definition of the Burgers vector in terms of the finite deformation theory. According to the state of the art of this theory, the total deformation gradient can be decomposed multiplicatively into elastic and plastic deformation sections. To be in agreement with the present notation, the multiplicative decomposition should be rewritten in the form

$$\mathbf{F}_{\mathrm{tot}} = \mathbf{F}\,\mathbf{F}_{\mathrm{pl}}. \tag{5}$$

As shown in Fig. 1, the integration of lattice distortions over Burgers circuits gives

$$\mathbf{b} = \oint_c d\mathbf{x} = \oint_O \mathbf{F}\, d\widehat{\mathbf{x}} = \oint_c (\mathbf{1} + \widehat{\boldsymbol{\beta}})\, d\widehat{\mathbf{x}}, \tag{6a}$$

$$-\widehat{\mathbf{b}} = \oint_C d\widehat{\mathbf{x}} = \oint_o \mathbf{F}^{-1} d\mathbf{x} = \oint_o (\mathbf{1} - \boldsymbol{\beta})\, d\mathbf{x}, \tag{6b}$$

where $\mathbf{b}$ and $\widehat{\mathbf{b}}$ are the the so-called spatial and true Burgers vectors, respectively, and c, C, o, O denote the open and closed Burgers circuits situated in the current (Eulerian) and reference (intermediate) configurations, respectively. It is worth emphasizing here that the lattice distortion $\boldsymbol{\beta}$ is related to lattice spacings in the current configuration. Alternatively, the distortions can be referred back to the spacings in a perfect lattice, and in this case the following transformation rule holds:

$$\widehat{\boldsymbol{\beta}} = (\mathbf{1} - \boldsymbol{\beta})^{-1} - \mathbf{1}. \tag{7}$$

Usually, in linear theory the differences between differentiation over the current, reference, and intermediate configurations are neglected, i.e., by assumption $(\partial \mathbf{u})/(\partial \mathbf{x}) \approx \partial \mathbf{u}/\partial \widehat{\mathbf{x}}$, $\widehat{\boldsymbol{\beta}} \approx \boldsymbol{\beta}$, $O \equiv o$, etc. Given this approach, a set of linear differential equations is obtained and many very useful analytical formulas can been derived.

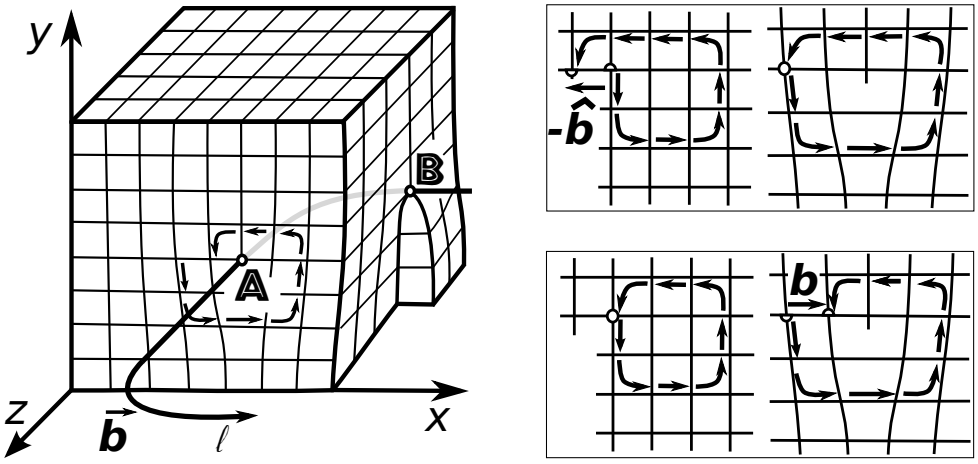

FIG. 1: An illustration of the true and spatial Burgers vectors and circuits.

2.2 Dislocation Density Tensor

Our notation refers back to the works by Kröner (1958, 1981, 1995), Teodosiu (1970, 1982), and de Wit (1970, 1981). Nevertheless, with respect to another convention used for the definition of the Burgers vector, cf. e.g., ours (2000, 2004) with Kröner's (1981), we find an opposite sign in some executive formulas. For instance, the use of the Stokes theorem gives

$$\mathbf{b} \stackrel{\mathrm{df}}{=} \oint_o \boldsymbol{\beta}\, d\mathbf{x} = \int_s \boldsymbol{\alpha}\, d\mathbf{s}, \tag{8}$$

where, according to the present notation, the dislocation density tensor is obtained as

$$\boldsymbol{\alpha} \stackrel{\mathrm{df}}{=} -\mathrm{curl}\boldsymbol{\beta}. \tag{9}$$

It can be shown that in the case of a straight-line dislocation, integration over the dislocation line direction gives

$$\mathbf{b} \otimes \mathbf{l} = \int_v \boldsymbol{\alpha}\, dv, \tag{10}$$

where $\mathbf{l} = \int_l d\mathbf{x}$ and $v = \int_s \int_l d\mathbf{x} \cdot d\mathbf{s}$. Equation (10) is very important for dislocation theory because it demonstrates the geometric meaning of the dislocation density tensor in relation to the Burgers vector and the dislocation line sense assumed by a given author.

A linear continuum theory of discrete dislocations is often found as a special case of a theory of residual stresses and elastic strain induced by certain crystallographic dislocations. In fact, even in the theory of discrete dislocations the displacement field still divides into elastic and plastic distortions. For example, in the case of a straight-line edge dislocation oriented as in Fig. 1 we find the following nonvanishing components of the dislocation density and plastic distortion tensors

$$\alpha_{\mathrm{pl}\,13} = b\,\delta(y)\,\delta(-x), \tag{11a}$$

$$\beta_{\mathrm{pl}\,12} = -b\,\delta(y)\,H(-x), \tag{11b}$$

where δ and H denote the Dirac and Heaviside functions, respectively. As a result, the integration of (2) along the Burgers circuit leads to

$$\oint_o d\mathbf{u}_{\mathrm{tot}} = \mathbf{0}, \tag{12a}$$

$$\oint_o \boldsymbol{\beta}\, d\mathbf{x} = \mathbf{b}, \tag{12b}$$

$$\oint_o \boldsymbol{\beta}_{\mathrm{pl}}\, d\mathbf{x} = -\mathbf{b}. \tag{12c}$$

2.3 Crystal Lattice Curvature

Similar to the partition of lattice distortions into the lattice rotation and elastic strain, the dislocation density tensor can be divided into the effect of lattice curvature and elastic strain gradient. Namely, application of the curl operator to (3) and the use of (9) leads to the compatibility condition

$$\boldsymbol{\alpha} = \boldsymbol{\alpha}_{\mathrm{w}} - \boldsymbol{\alpha}_{\mathrm{e}}, \tag{13}$$

where

$$\boldsymbol{\alpha}_{\mathrm{w}} \stackrel{\mathrm{df}}{=} -\mathrm{curl}\,\mathbf{w}, \tag{14a}$$

$$\boldsymbol{\alpha}_{\mathrm{e}} \stackrel{\mathrm{df}}{=} -\mathrm{curl}\,\boldsymbol{\varepsilon}. \tag{14b}$$

In Nye (1953) noted that if the lattice curvature tensor is defined as a gradient of the vector of crystal lattice rotation, $\boldsymbol{\kappa} \stackrel{\mathrm{df}}{=} \mathrm{grad}\,\boldsymbol{\phi}$, and $\mathbf{w}$ is a multivector $w_{ij} \stackrel{\mathrm{df}}{=} e_{ijk}\phi_k$, then the following relationship holds:

$$\begin{aligned}(\mathrm{curl}\,w)_{il} &= w_{ij,m}e_{jml} = \phi_{k,m}e_{kij}e_{jml} \\ &= \phi_{k,m}(\delta_{km}\delta_{il} - \delta_{kl}\delta_{im}) = -\phi_{l,i} + \phi_{k,k}\delta_{il}.\end{aligned} \tag{15}$$

In view of (14b), this leads to the mutually invertible relationship between $\boldsymbol{\kappa}$ and $\boldsymbol{\alpha}_{\mathrm{w}}$

$$\boldsymbol{\alpha}_{\mathrm{w}} = -\boldsymbol{\kappa}^T + \mathrm{tr}\,\boldsymbol{\kappa}^T, \quad \boldsymbol{\kappa} = -\boldsymbol{\alpha}_{\mathrm{w}}^T + \frac{1}{2}\,\mathrm{tr}\,\boldsymbol{\alpha}_{\mathrm{w}}^T, \tag{16}$$

where tr means the trace of a given tensor, i.e., $[\mathrm{tr}\,\boldsymbol{\alpha}] = \begin{bmatrix} \mathrm{tr}\alpha & \cdot & \cdot \\ \cdot & \mathrm{tr}\alpha & \cdot \\ \cdot & \cdot & \mathrm{tr}\alpha \end{bmatrix}$, and $\mathrm{tr}\,\alpha = \alpha_{11} + \alpha_{22} + \alpha_{33}$.

By analogy to (13) the total lattice curvature can be divided uniquely into the elastic and plastic curvature

$$\boldsymbol{\kappa} = \boldsymbol{\kappa}_{\mathrm{e}} + \boldsymbol{\kappa}_{\mathrm{pl}}, \tag{17}$$

where

$$\boldsymbol{\kappa}_{\mathrm{e}} \stackrel{\mathrm{df}}{=} -\boldsymbol{\alpha}_{\mathrm{e}}^T + \frac{1}{2}\,\mathrm{tr}\,\boldsymbol{\alpha}_{\mathrm{e}}^T, \text{ and } \boldsymbol{\kappa}_{\mathrm{pl}} \stackrel{\mathrm{df}}{=} -\boldsymbol{\alpha}^T + \frac{1}{2}\,\mathrm{tr}\,\boldsymbol{\alpha}^T. \tag{18}$$

Unfortunately, with respect to possible nonzero axiators of $\boldsymbol{\alpha}_{\mathrm{e}}$ and $\boldsymbol{\alpha}$, the relationship is not invertible, and in general, cf. (16)

$$\boldsymbol{\alpha}_{\mathrm{e}} \neq -\boldsymbol{\kappa}_{\mathrm{e}}^T + \mathrm{tr}\,\boldsymbol{\kappa}_{\mathrm{e}}^T, \quad \text{and} \quad \boldsymbol{\alpha} \neq -\boldsymbol{\kappa}_{\mathrm{pl}}^T + \mathrm{tr}\,\boldsymbol{\kappa}_{\mathrm{pl}}^T. \tag{19}$$

Summing up, among all families of the $\boldsymbol{\alpha}_{\ldots}$ and $\boldsymbol{\kappa}_{\ldots}$ tensors discussed above, only two tensors, $\boldsymbol{\alpha}_{\mathrm{w}}$ and $\boldsymbol{\kappa}$, compose a pair of mutually equivalent tensor measures in the sense suggested by Nye. It is worth emphasizing that from a crystallographic point of view, $\boldsymbol{\alpha}_{\mathrm{w}}$ does not represent any measure of dislocation density, and in the extreme case, the lattice curvature tensor can even vanish

in the presence of dislocation field (see Fig. 2c). The geometric meaning of the division of the lattice distortion field into a few different elastic strains and lattice curvature modes is shown schematically in Fig. 2. As is shown in the Appendix, a simple-shear mode does not correspond to $\boldsymbol{\alpha}_{\mathrm{w}} = \mathbf{0}$ but to a mixed mode in which $\boldsymbol{\alpha}_{\mathrm{e}} = \frac{1}{2}\boldsymbol{\alpha}$ and $\boldsymbol{\alpha}_{\mathrm{w}} = \frac{1}{2}\boldsymbol{\alpha}$. In the similar way it can be shown that in a pure shearing mode, in which the lattice rotation field vanishes, the slip plane considered is not flat but deviates proportionally to the elastic strain, (cf. Fig. 2c). The reason is that the lattice rotation tensor does not represent any rotation of a given crystal slip plane but corresponds to a mean rotation of all material directions crossing a given material point.

Similarly to $\boldsymbol{\alpha}$, the Burgers vector can also be divided into the effect of the lattice curvature and elastic strain according to

$$\mathbf{b} = \mathbf{b}_{\mathrm{w}} + \mathbf{b}_{\mathrm{e}}, \tag{20}$$

where

$$\begin{aligned} \mathbf{b}_{\mathrm{w}} &\overset{\mathrm{df}}{=} \oint_o \mathbf{w}\, d\mathbf{l} = \int_s \boldsymbol{\alpha}_{\mathrm{w}}\, d\mathbf{s}, \\ \mathbf{b}_{\mathrm{e}} &\overset{\mathrm{df}}{=} \oint_o \boldsymbol{\varepsilon}\, d\mathbf{l} = \int_s \boldsymbol{\alpha}_{\mathrm{e}}\, d\mathbf{s}. \end{aligned} \tag{21}$$

2.4 Compatibility Conditions and Residual Stresses

Application of the curl operator to (2) gives a very important compatibility condition between the lattice and plastic distortions,

$$-\operatorname{curl}\boldsymbol{\beta} = \operatorname{curl}\boldsymbol{\beta}_{\mathrm{pl}}, \tag{22}$$

The dislocation density tensor field $\boldsymbol{\alpha}(\mathbf{x})$ induced by plastic deformation $\boldsymbol{\beta}_{\mathrm{pl}}(\mathbf{x})$ can be treated as a source field for residual stresses. Then the use of (35) allows the compatibility condition to be rewritten in the form

$$\operatorname{curl}\boldsymbol{\beta} = \boldsymbol{\alpha}(\mathbf{x}), \tag{23}$$

The condition is composed of nine mutually independent differential equations. Contrary to discrete dislocations, *the residual stresses are not an inherent part of the continuous field of dislocations* $\boldsymbol{\alpha}(\mathbf{x})$. For example, it can be shown that in a plastic bending mode shown schematically in Fig. 2a, the elastic continuum is in a residual-stress-free configuration. Fortunately, it appears that a tensor measure being sufficient to state a residual stress problem in the form of a differential equation set is grad$\boldsymbol{\alpha}$. Moreover, it can be shown that some of its components do not affect residual stress, e.g., a continuous dislocation field composing a tilt grain boundary is found to be a stress-free configuration. Such properties of the gradient became the reason to introduce another group of tensor measures of lattice distortion incompatibility, namely,

$$\boldsymbol{\eta} \overset{\mathrm{df}}{=} \operatorname{inc}\boldsymbol{\beta},\ \ \boldsymbol{\eta}_{\mathrm{e}} \overset{\mathrm{df}}{=} \operatorname{inc}\boldsymbol{\varepsilon},\ \ \boldsymbol{\eta}_{\mathrm{w}} \overset{\mathrm{df}}{=} \operatorname{inc}\mathbf{w}. \tag{24}$$

A linear operator of the incompatibility holds the symmetry of the input tensor field, and according to (3)

$$\boldsymbol{\eta} = \boldsymbol{\eta}_{\mathrm{e}} + \boldsymbol{\eta}_{\mathrm{w}}. \tag{25}$$

The incompatibility tensor was introduced for the elastic strain in its original form by Kröner (1955). In the present notation the measure introduced by Kröner corresponds to $\boldsymbol{\eta}_{\mathrm{e}}$. His intention was to introduce a strain compatibility condition in the analogical form as it is found in the classical theory of elasticity, inc$\boldsymbol{\varepsilon} = \mathbf{0}$. Unfortunately, in the continuum theory of dislocations, the vanishing of residual stresses does not mean yet the material is free of dislocations. For example, in the case of a lattice bending mode shown in Fig. 2, the elastic strain vanishes while the lattice rotation field corresponds to the axisymmetric curved lattice. In such a case, it is easy to show that for an arbitrary chosen Burgers circuit, the resultant Burgers vector does not vanish according to (3), (6), and (7).

In this paper we discuss only the first-grade (classical) continuum with the symmetric Cauchy stress tensor and

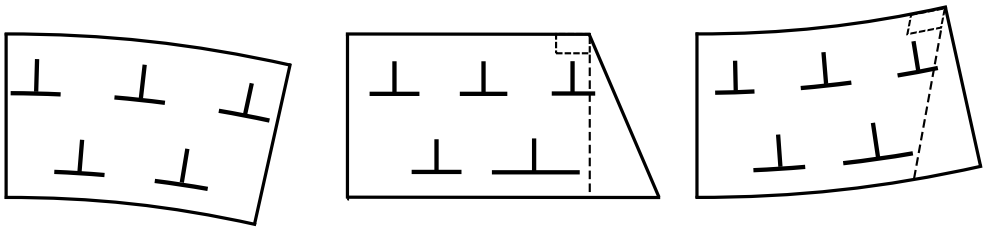

FIG. 2: Dislocations in different lattice distortion modes. From left-to-right: lattice bending, simple shearing, and pure shearing.

none of the momentum stresses. Limiting our consideration to elastostatics, the stress balance equation together with the compatibility condition and Hooke's law state a closed $3+6+6$ equations set

$$\operatorname{div}\boldsymbol{\sigma}=\mathbf{0}, \tag{26a}$$

$$\operatorname{inc}\boldsymbol{\varepsilon}=\boldsymbol{\eta}_{\mathrm{e}}, \tag{26b}$$

$$\boldsymbol{\sigma}=\mathbf{c}:\boldsymbol{\varepsilon}, \tag{26c}$$

for fifteen wanted variables: $3\times u_i+6\times\varepsilon_{ij}+6\times\sigma_{ij}$. The middle equation comprises a subset of six differential equations for six components of $\boldsymbol{\varepsilon}$. Therefore, ignoring the remaining upper/lower equations one can solve the subset independently. Nevertheless, strain fields obtained in this way do not compose a total strain but only its incompatible part, $\boldsymbol{\varepsilon}^{\mathrm{inc}}$. Note that the mentioned strain compatibility equation is second order, and therefore its general integral can be appended by an arbitrarily chosen, self-compatible strain field, according to

$$\boldsymbol{\varepsilon}=\boldsymbol{\varepsilon}^{\mathrm{inc}}+\frac{1}{2}\big(\operatorname{grad}\mathbf{u}+\operatorname{grad}^{T}\mathbf{u}\big). \tag{27}$$

In other words, to find a total strain one still needs to solve the stress equilibrium equation, and the same situation is true of the lattice rotation. Namely, in solving (26), only the compatible part of the rotation tensor yield from the displacement field can be obtained, whereas the Burgers vector remains undetermined as long as the lattice orientation incompatibility tensor field is fixed. Therefore, to find the total lattice rotation

$$\mathbf{w}=\mathbf{w}^{\mathrm{inc}}+\frac{1}{2}\big(\operatorname{grad}\mathbf{u}-\operatorname{grad}^{T}\mathbf{u}\big), \tag{28}$$

one also needs to solve three independent differential equations for the source field $\boldsymbol{\eta}_{\mathrm{w}}(\mathbf{x})$. Thus, as a minimal equation set to determine a set of variables $\boldsymbol{\sigma},\boldsymbol{\varepsilon}$, $\mathbf{w}$, and $\mathbf{u}$, we have

$$\operatorname{div}\boldsymbol{\sigma}=\mathbf{0}, \tag{29a}$$

$$\operatorname{inc}(\boldsymbol{\varepsilon}+\mathbf{w})=\boldsymbol{\eta}, \tag{29b}$$

$$\boldsymbol{\sigma}=\mathbf{c}:\boldsymbol{\varepsilon}. \tag{29c}$$

where $\boldsymbol{\eta}=-(\operatorname{curl}\boldsymbol{\alpha}^{T})^{T}$. Otherwise, in solving only (26), the lattice distortions will remain undetermined. An advantage of (29) over (26) is the possibility to state more flexible boundary conditions, namely, the Neumann boundary conditions for (29b), which corresponds to the dislocation traction $\mathbf{t}_{\alpha}=-\mathbf{n}\times\boldsymbol{\alpha}^{T}$, where $\mathbf{n}$ is the unit normal to the boundary. In the first case, in solving only (26) two mutually independent boundary conditions for traction must be imposed subsequently: in the first step for the elastic strain, and in the second step for the lattice curvature.

3. ANALYTICAL EQUATIONS FOR MIXED STRAIGHT DISLOCATION

The displacement field around a mixed straight-line dislocation in an elastic material is defined by the classical formulas which refer back to the works of Love (1927) and Read, Jr. (1953):

$$u_x=\frac{b_x}{2\pi}\left(\arctan\frac{y}{x}+\frac{xy}{2(1-\nu)(x^2+y^2)}\right)-\frac{b_x}{2}, \tag{30a}$$

$$u_y=-\frac{b_x}{2\pi}\left(\frac{1-2\nu}{4(1-\nu)}\ln(x^2+y^2)+\frac{x^2-y^2}{4(1-\nu)(x^2+y^2)}\right), \tag{30b}$$

$$u_z=\frac{b_z}{2\pi}\arctan\frac{y}{x}-\frac{b_z}{2}. \tag{30c}$$

where the edge and screw components of the Burgers vector, b_x and b_z, are parallel to the x and z axes, respectively (see Fig. 1). Nonvanishing components of lattice distortions are

$$\beta_{xx}=-\frac{b_x}{2\pi}\frac{(3-2\nu)x^2y+(1-2\nu)y^3}{2(1-\nu)(x^2+y^2)^2}, \tag{31a}$$

$$\beta_{xy}=\frac{b_x}{2\pi}\frac{(3-2\nu)x^3+(1-2\nu)xy^2}{2(1-\nu)(x^2+y^2)^2}, \tag{31b}$$

$$\beta_{yx}=-\frac{b_x}{2\pi}\frac{(1-2\nu)x^3+(3-2\nu)xy^2}{2(1-\nu)(x^2+y^2)^2}, \tag{31c}$$

$$\beta_{yy}=\frac{b_x}{2\pi}\frac{(1+2\nu)x^2y-(1-2\nu)y^3}{2(1-\nu)(x^2+y^2)^2}, \tag{31d}$$

$$\beta_{zx}=-\frac{b_z}{2\pi}\frac{y}{x^2+y^2}, \tag{31e}$$

$$\beta_{zy}=\frac{b_z}{2\pi}\frac{x}{x^2+y^2}, \tag{31f}$$

3.1 Atomistic Reconstruction of Dislocations

In many cases the analytical solutions obtained by means of the linear theory of dislocations are used to generate the input files for atomistic modeling of the physical properties of dislocation cores. In the case of the wurtzite structure of GaN, such a method has been used in many papers starting from Béré and Serra (2002). The structure of such obtained cores depends on which coordinates the dislocation center takes in the unit crystal cell, as shown in Fig. 3.

The dislocation cores generated by the use of (30) do not hold symmetry of atomic bonds distribution. To avoid

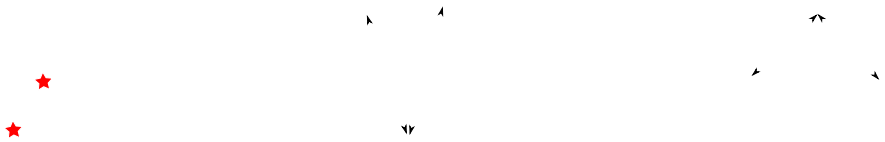

FIG. 3: Dislocation core structures generated by means of Eq. (30) for $\mathbf{b} = \frac{1}{3}\langle 2\bar{1}\bar{1}0\rangle$ in GaN.

the asymmetry, some modification into (30) was considered by de Wit (1973), cf. Lymperakis (2005). Nevertheless, to obtain a symmetric distribution we should apply finite deformation theory in which the differences between the differentiation over the reference and spatial configurations are taken into account. The problem is that strict analytical solutions based on the nonlinear theory have not been obtained for most of the typical problems for dislocations, as yet.

3.2 Distortion Distribution Inside the Core

In the origin of the coordinate system $\{x, y, z\}$ the analytical functions (31) are singular. This causes many problems in the numerical modeling of dislocation properties. In order to remove this singularity, let us replace $\beta(x, y, z)$ by a second set of smooth functions $\beta^c(x, y, z)$, which by assumption should satisfy some geometrical conditions. For this aim let us assume that the core occupies a conventional region $x^2 + y^2 < r_\circ^2$, where $r_\circ$ is the dislocation core radius. Usually, in practical applications it is assumed $\frac{1}{2}b \geq r_\circ \geq 100b$. Let the wanted function $\beta^c(x, y, z)$ hold the following conditions:

Inside the core:

1. *The distortion field substituted into Hooke's law holds the stress equilibrium condition*

$$\operatorname{div} \boldsymbol{\sigma} = 0, \tag{32a}$$

2. *The dislocation field obtained as* $\boldsymbol{\alpha} = -\operatorname{curl} \boldsymbol{\beta}^c$ *is axisymmetric*

$$\boldsymbol{\alpha} = \boldsymbol{\alpha}(r), \tag{32b}$$

where $r \stackrel{\text{df}}{=} \sqrt{x^2 + y^2}$.

3. *Similar to the integral condition* $[\mathbf{b}_\text{e}] = [b_x, 0, b_z]^T$, *the dislocation tensor field satisfies the analogical strict condition*

$$[\boldsymbol{\alpha}] = \alpha_{xz} \begin{bmatrix} 0 & 0 & 1 \\ 0 & 0 & 0 \\ 0 & 0 & \frac{b_x}{b_z} \end{bmatrix}. \tag{32c}$$

4. *The distortion functions* $\boldsymbol{\beta}^c(x, y, z)$ *are polynomials of the lowest possible order as needed to fulfill all the conditions above.*

On the border of the dislocation core:

5. *The distortion tensor field and its gradient are continuous,*

$$\boldsymbol{\beta}^c\big|_{x^2+y^2=r_\circ^2} = \operatorname{grad} \mathbf{u}, \tag{32d}$$

$$\operatorname{grad} \boldsymbol{\beta}^c\big|_{x^2+y^2=r_\circ^2} = \operatorname{grad}^2 \mathbf{u}, \tag{32e}$$

6. *The distortion incompatibility tensor vanishes,*

$$\operatorname{inc} \boldsymbol{\beta}^c\big|_{x^2+y^2=r_\circ^2} = 0. \tag{32f}$$

A result arising from the last condition is that the wanted distortion function is not only C^1 class, but also, some linear combination of its second gradient must vanish on the border of the dislocation core. It can be shown that (32b) and (32c) lead to the following form of the incompatibility tensor:

$$[\boldsymbol{\eta}] = \alpha_{xz,r} \begin{bmatrix} -\frac{b_x}{b_z} y & 0 & 0 \\ \frac{b_x}{b_z} x & 0 & 0 \\ y & 0 & 0 \end{bmatrix}, \tag{33}$$

where $\alpha_{xz,r}$ means the covariant derivative of α_{xz} over its radial coordinate. It can be demonstrated that the substitution of (33) into (29) under (32) gives the following distortion functions inside the core:

$$\beta^c_{xx} = \frac{b_x}{4\pi(1-\nu)r_\circ^6}\Big[\big(-3r_\circ^4 y+3r_\circ^2 y^3-y^5\big)(1-2\nu) + x^2\left(-3r_\circ^2 y+2y^3\right)(1+2\nu)+x^4 y\,(3+2\nu)\Big], \tag{34a}$$

$$\beta^c_{xy} = \frac{b_x}{4\pi(1-\nu)r_\circ^6}\Big\{x\Big[\,(9-6\nu)\,r_\circ^4-(15-6\nu)\,r_\circ^2 y^2 +(7-2\nu)\,y^4\Big]+x^3\Big[(-9+6\nu)r_\circ^2+(10-4\nu) \times y^2\Big] + x^5\,(3-2\nu)\Big\}, \tag{34b}$$

$$\beta^c_{yx} = \frac{b_x}{4\pi(1-\nu)r_\circ^6}\Big\{x\Big[(18\nu-15)r_\circ^4+(21-30\nu) \times r_\circ^2 y^2+(14\nu-9)y^4\Big]+x^3\Big[(27-30\nu)r_\circ^2 + (28\nu-22)y^2\Big] + x^5(14\nu-13)\Big\}, \tag{34c}$$

$$\beta^c_{yy} = \frac{b_x}{4\pi(1-\nu)r_\circ^6}\Big\{\Big[(18\nu-9)r_\circ^4 y+(15-30\nu) \times r_\circ^2 y^3+(14\nu-7)y^5\Big] + x^2\Big[(21-30\nu)r_\circ^2 y + (28\nu-18)y^3\Big] + x^4(14\nu-11)y\Big\}, \tag{34d}$$

$$\beta^c_{zx} = \frac{b_z}{2\pi r_\circ^6}\Big[-3r_\circ^4 y+3r_\circ^2 y^3-y^5 + x^2\left(3r_\circ^2 y-2y^3\right)-x^4 y\Big], \tag{34e}$$

$$\beta^c_{zy} = \frac{b_z}{2\pi r_\circ^6}\Big[x\left(3r_\circ^4-3r_\circ^2 y^2+y^4\right) + x^3\left(-3r_\circ^2+2y^2\right)+x^5\Big]. \tag{34f}$$

This corresponds to the following distribution of the dislocation field in the core:

$$\alpha_{xz} = \frac{3b_x}{\pi r_\circ^6}(r_\circ^2-x^2-y^2)^2, \tag{35a}$$

$$\alpha_{zz} = \frac{3b_z}{\pi r_\circ^6}(r_\circ^2-x^2-y^2)^2, \tag{35b}$$

and the following residual stresses:

$$\sigma^c_{xx} = \frac{b_x\mu}{2\pi(1-\nu)r_\circ^6}\Big\{-3yr_\circ^4(1+2\nu)+3y^3r_\circ^2 \times(1+4\nu)-y^5(1+6\nu)-x^2\Big[3yr_\circ^2(1-4\nu) - 2y^3(1-6\nu)\Big]+3x^4y(1-2\nu)\Big\}, \tag{36a}$$

$$\sigma^c_{yy} = \frac{b_x\mu}{2\pi(1-\nu)r_\circ^6}\Big\{-3yr_\circ^4(3-2\nu)+3y^3r_\circ^2 \times(5-4\nu)-y^5(7-6\nu)+x^2\Big[3yr_\circ^2(7-4\nu) - 6y^3(3-2\nu)\Big]-x^4y(11-6\nu)\Big\}, \tag{36b}$$

$$\sigma^c_{zz} = \frac{b_x\mu\nu}{\pi(1-\nu)r_\circ^6}\Big[-6yr_\circ^4+9y^3r_\circ^2-4y^5 + x^2(9yr_\circ^2-8y^3)-4yx^4\Big], \tag{36c}$$

$$\sigma^c_{yz} = \frac{b_z\mu}{2\pi r_\circ^6}\Big[x(3r_\circ^4-3r_\circ^2y^2+y^4)-x^3 \times\left(3r_\circ^2-2y^2\right)+x^5\Big], \tag{36d}$$

$$\sigma^c_{zx} = \frac{b_z\mu}{2\pi r_\circ^6}\Big[-3r_\circ^4y+3r_\circ^2y^3-y^5+x^2 \times\left(3r_\circ^2y-2y^3\right)-x^4y\Big], \tag{36e}$$

$$\sigma^c_{xy} = \frac{b_x\mu}{2\pi(1-\nu)r_\circ^6}\Big\{x\Big[-3(1-2\nu)r_\circ^4+3(1-4\nu) \times r_\circ^2y^2-(1-6\nu)y^4\Big]+x^3\Big[3(3-4\nu)r_\circ^2 - 6(1-2\nu)y^2\Big]-x^5(5-6\nu)\Big\}. \tag{36f}$$

where μ and ν are the shear modulus and Poisson's ratio, respectively.

The integration of the strain energy density gives the following formula for the energy stored per unit length L of the dislocation core:

$$\frac{W_c}{L} = \mu b^2\big[73(1-\nu)^2\cos^2\beta+\big(97-199\nu + 72\nu^2\big)\sin^2\beta\big]/480\pi(1-\nu^2). \tag{37}$$

It is worth emphasizing that such obtained dislocation core energy is independent of the size of the core assumed. Obviously, this surprising mathematical result does not yet mean that the total strain energy introduced by the continuously distributed dislocation core is independent of its size. As a matter of fact, by increasing the radius of the dislocation core we decrease the energy stored outside the dislocation core, and this means that the resultant total elastic strain energy is sensitive to the core radius assumed, according to

$$\frac{W}{L} = \frac{\mu b^2}{4\pi}\left[\left(\cos^2\beta+\frac{\sin^2\beta}{1-\nu}\right)\ln\frac{R}{r_\circ} + \frac{73(1-\nu)^2\cos^2\beta+(97-199\nu+72\nu^2)\sin^2\beta}{120(1-\nu^2)}\right], \tag{38}$$

where R is the external radius corresponding to the size of the crystal region considered [cf. Eq. (3.87) in Hirth and Lothe (1982)].

4. NUMERICAL EXAMPLE

As was shown in Section 3.1, the analytical equations obtained in the theory of discrete dislocations are very useful for the generation of input files for the atomistic modeling of dislocations. Nevertheless, in the numerical methods based on continuum mechanics, such as the finite element (FE) and finite difference methods, serious numerical problems arise from the the singularity of the stress/strain fields resulting from the discrete character of dislocations assumed. To overcome this a mixed analytical-FE formulation oriented on modeling of singularities has been developed by preparing special FEs with singular shape functions in the center of the dislocation core [see Stigh (1993)].

In the present paper another method based on the finite deformation approach is used (Dłuzewski et al., 2004). To use the method authors needed to extract the lattice distortion map by means of the computer image processing of the HRTEM image of the investigated sample (Hÿtch, 1998; Kret et al., 2003). Unfortunately, such an approach can be used only if the quality of the image is relatively good. In Fig. 4 an HRTEM image of the GaN sample is shown. Its quality is sufficiently good to identify the dislocations on the image, but in some regions the bright dots have insufficient contrast to extract the distortion tensor maps by means of computer processing of the image. Therefore, in the present paper the role of tensor fields obtained from HRTEM image processing has be taken by analytical Eq. (34). The fields (31) outside and (34) inside of dislocation cores have to be superposed for sequential dislocations to obtain a resultant distortion field,

$$\boldsymbol{\beta}(\mathbf{x}) = \sum_i \begin{cases} \boldsymbol{\beta}^c(\mathbf{x}-\mathbf{x}_i) & \text{for} \quad (\mathbf{x}-\mathbf{x}_i)^2 < r_\circ, \\ \boldsymbol{\beta}(\mathbf{x}-\mathbf{x}_i) & \text{for} \quad (\mathbf{x}-\mathbf{x}_i)^2 \geq r_\circ, \end{cases} \tag{39}$$

where $\mathbf{x}_i$ and $r_\circ$ denote the position of the the ith dislocation core and assumed dislocation core radius, respectively. It was assumed that three among the dislocations visible on the HRTEM image are edge $\frac{1}{3}\langle 2\bar{1}\bar{1}0\rangle$ and one is

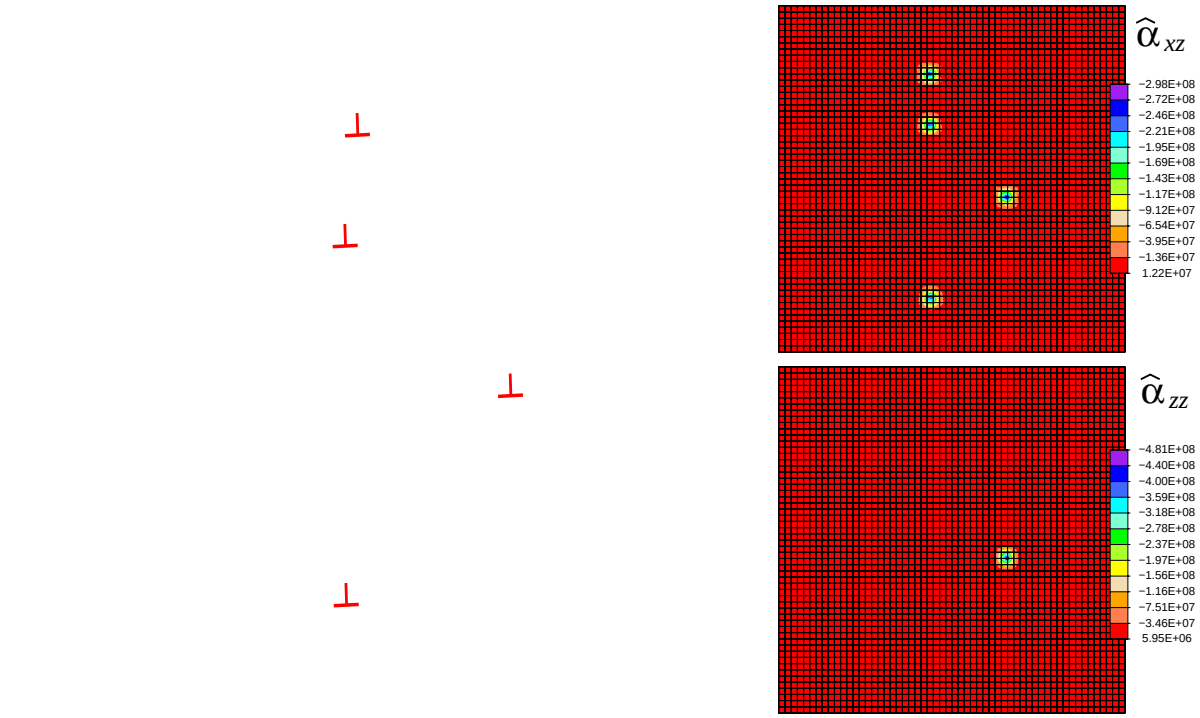

FIG. 4: HRTEM image of GaN sample, viewed along [0001], on which four dislocations are marked, and the edge and screw components of the dislocation tensor field, $\widehat{\alpha}_{xz}$ and $\widehat{\alpha}_{zz}$, preprocessed by means of Eq. (39) for FE calculations.

mixed $\frac{1}{3}\langle 2\bar{1}\bar{1}3\rangle$, which corresponds to $b_x = a$ and $b_z = c$, where a and c denote the lattice constants of the trigonal crystal symmetry system (see Table 2). According to the derived Eq. (34) the magnitude of the dislocation core radius can be chosen arbitrarily. In other words, an arbitrarily chosen cylindrical region with a singularity can be cutout and replaced by a continuous stress/distortion tensor field which satisfies the six conditions discussed in Section 3.2. In the case considered here, $r_\circ$ was chosen to be equal to the length of two cubic finite elements. From a crystallographic point of view this corresponds to $r_\circ = 1.5\,a$.

The constitutive model used is in the nonlinear FE code based on the anisotropic hyperelasticity and Hencky strain measure (Dłuzewski, 2000). The FE code used is dedicated to the modeling of dislocations in semiconductor heterostructures [see Dłuzewski et al. (2004)]. The lattice distortion field (39) has been translated to the local relaxed configuration, according to (7). The material parameters for dislocations in GaN were assumed to be the same as those used by Young et al. (2007) (see Table 2). A stress-free boundary condition was used to demonstrate the residual stresses induced by dislocations (see Fig. 5).

5. CONCLUSIONS

In this paper a new analytical solution was derived and presented within the framework of the continuum theory of dislocations [see Eqs. (34–38)]. The equations concern the linear theory of a continuously distributed dislocation core. In order to solve the nonlinear boundary-value problem for dislocations the distortion field (39) was used as the input data to solve an FE problem stated for dislocations in an anisotropic hyperelastic continuum. As an example, the residual stress/distortion fields corresponding to dislocations visible on the HRTEM image of a GaN sample were solved. Independently of this fully continuous approach, the linear continuum theory of discrete dislocations was discussed in terms of artifacts in the reconstruction of dislocation cores.

In the literature many analytical solutions for the elastic strain/stress fields induced by dislocations are published. In the present paper a complete solution has been given, not only for the strain and stress but also for lattice rotation. Both parts of the lattice distortions, the symmetric and antisymmetric, take the same important role in reconstruction of atomistic models of dislocations, and

TABLE 2: Empirical constants used in this work. Units are in nanometers, gigapascals, or are dimensionless.

ν	μ	a	c	C_{11}	C_{12}	C_{13}	C_{33}	C_{44}
0.35	124	0.31466	0.519	396	137	108	373	116

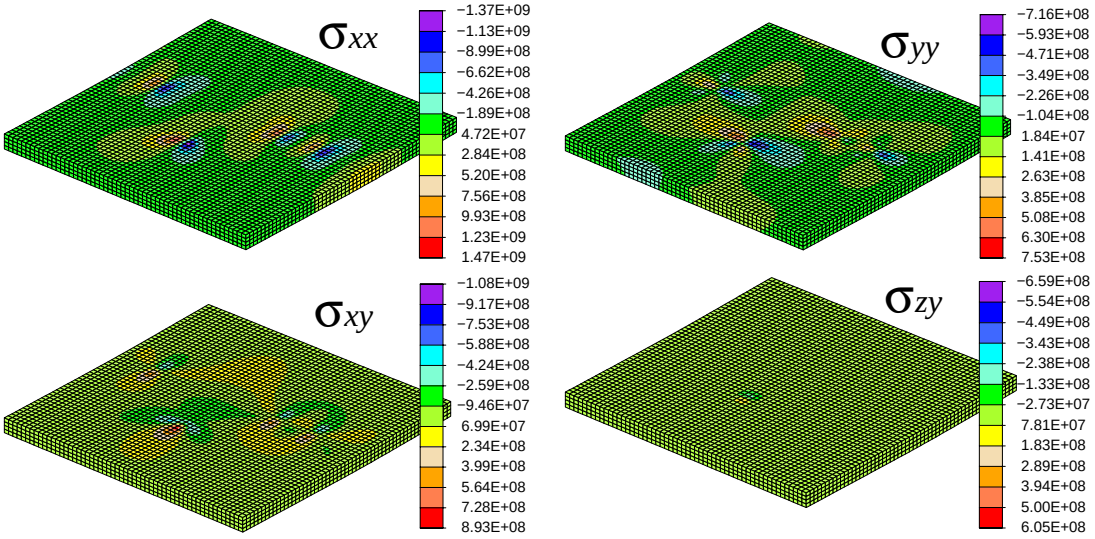

FIG. 5: The Cauchy stress field obtained in the nonlinear FEM based on the use of the continuum theory of dislocations.

only both together give the unique transition to the finite deformation approach. It is easy to show that if the lattice distortion is given then the elastic stretch as well as the orthogonal tensor of lattice rotation can be reconstructed uniquely. Contrary to that, if only the infinitesimal strain field $\boldsymbol{\varepsilon}(\mathbf{x})$ is given, no unique atomistic reconstruction nor any transition to the finite deformation theory is possible.

The main disadvantage of the new analytical solution is it is composed of two different analytical functions coinciding on the Burgers circuit. Its radius can be fit arbitrarily as the core radius. Such like methods are widely used [see, for example, the review in Cai et al. (2006)]. The present approach, as in many others from the group based on the cutoff technique, allows all the advantages of a discrete character of dislocations to be saved and extends its application to some practical solutions only for the dislocation core. For example, the important advantage of the classical solution is a discrete character of dislocation resulting from the localization of plastic distortions to a jump on a slip or climb plane [cf. Eq. (30a)]. As shown in Fig. 3, thanks to such a discrete jump, the core structure can be reconstructed in atomistic manner. The resultant form of dislocation core obtained depends on the reference position of the dislocation center taken in a perfect unit cell. Use of the present continuum model of dislocation still allows unique reconstruction of the lattice structure outside the core, while inside, the atomic positions are no longer unique as the lattice displacement field is not unique in the case of a continuously distributed dislocation tensor field. In these terms the continuum field theory can be treated as a theory in which the dislocation tensor field takes a role of distribution of a probability were the dislocation center is at a given moment.

Contrary to the continuum theory of discrete dislocations, the residual stresses are not an inherent part of a continuously distributed dislocation tensor field. Therefore, appending the elastic strain field by a different rotation field such as that obtained in the lattice distortion field can correspond to quite different dislocations understood in the crystallographic sense of integration over the Burgers circuit. In other words, contrary to discrete dislocations, any analytical solution given only for elastic strain/stress fields is undetermined as long as the rotation field is not uniquely fixed.

ACKNOWLEDGMENTS

This research was carried out within the framework of the European Commission PARSEM project MRTN-CT-2004-005583 and additionally subsidized by the Ministry of Science and Higher Education (MSHE) in Poland, grant no. 131/6PREU/2005/7, in the period 1 Mar 2006 – 28 Feb 2009. Since 1 Mar 2009 the investigations continued within grant no. 0634/R/T02/2007/02 founded by MSHE.

REFERENCES

Béré, A. and Serra, A. Atomic structure of dislocation cores in GaN. *Phys. Rev. B*, vol. **65**, p. 205323, 2002.

Bilby, B. A. Continuous distribution of dislocations, in Sneddon, I. and Hill, R., Eds., *Progress in Solid Mechanics*, vol. **1**, pp. 331–398, Amsterdam, North-Holland, 1960.

Cai, W., Arsenlis, A., Weinbergera, C. R., and Bulatov, V. V., A non-singular continuum theory of dislocations. *J. Mech. Phys. Solids*, vol. **54**, pp. 561–587, 2006.

de Wit, R., *The continuum theory of stationary dislocations*, vol. **10**, *Advances in Solid State Physics*, New York: Academic Press, 1960.

de Wit, R., Linear theory of static disclinations, in Simmonds, J., de Wit, R., and Bullough, R., Eds., *Fundamentals Aspects of Dislocations*, pp. 651–673, *National Burureau of Standards Special Publication 317*, vol. **II**, 1970.

de Wit, R., Theory of dislocations II, Continuous and discrete dislocations in anisotropic elasticity, *J. Res. Nat. Bur. Stand. (USA) — A. Phys. Chem.*, vol. **77A**, p. 608, 1973.

de Wit, R., A view of the relation between the continuum theory of lattice defects and non-Euclidean geometry in the linear approximation. *Int. J. Eng. Sci.*, vol. **19**(12), pp. 1475–1506, 1981.

Dłużewski, P., Anisotropic hyperelasticity based upon general strain measures. *J. Elasticity*, vol. **60**(2), pp. 119–129, 2000.

Dłużewski, P., Maciejewski, G., Jurczak, G., Kret, S., and Laval, J.-Y., Nonlinear FE analysis of residual stresses induced by misfit dislocations in epitaxial layers, *Comput. Mater. Sci.*, vol. **29**(3), pp. 379–395, 2004.

Gairola, B. K. D., Nonlinear elastic problems, in Nabaro, F., editor, *Dislocations in Solids*, vol. **1**, pp. 223–342, Amsterdam: North-Holland, 1979.

Hirth, J. P. and Lothe, J., *Theory of Dislocations*, Wiley, New York, 1982.

Hÿtch, M. J., Quantitative analysis of strain field in thin films from HRTEM micrographs, *Thin Solid Films*, vol. **319**, pp. 157–162, 1998.

Kondo, K., On geometrical and physical foundations of the theory of yielding, in *Proc. 2nd Japan Nat. Congr. Appl. Mech*, vol. **2**, pp. 41–47, 1952.

Kondo, K., Non-Riemannian and Finslerian approaches to the theory of yielding, *Int. J. Eng. Sci.*, vol. **1**, pp. 71–88, 1963.

Kret, S., Dłużewski, P., and Laval, J.-Y., On the measurement

of dislocation cores distribution in GaAs/ZnTe/CdTe heterostructure by transmission electron microscopy, *Philos. Mag. A*, vol. **83**, pp. 231–244, 2003.

Kröner, E., Die inneren Spannungen und der Inkompatibilitätstensor in der Elastizitätstheorie, *Z. Angew. Phys.*, vol. **7**, pp. 249–257, 1955.

Kröner, E., *Kontinuumstheorie der Vesetzungen und Eigenspannungen*, Berlin: Springer Verlag, 1958.

Kröner, E., Continuum theory of defects, in Balian, R., Kleman, M., and Poiries, J.-P., Eds., *Physics of Defects*, pp. 215–315, Amsterdam: North-Holland, 1981.

Kröner, E., Dislocations in crystals and in continua: A confrontation, *Int. J. Eng. Sci.*, vol. **33**(15), pp. 2127–2135, 1995.

Love, A. E. H., *Mathematical Theory of Elasticity*, Cambridge: Cambridge University Press, 1927.

Lymperakis, L., *Ab-Initio Based Multiscale Calculations of Extended Defects in and on Group III – Nitrides*, PhD Thesis, Department Physik der Fakultät für Naturwissenschaften an der Universität Paderborn, 2005.

Nye, J. F., Some geometrical relations for dislocated crystals, *Acta Metallurgica*, vol. **1**, pp. 153–162, 1953.

Read Jr., W. T., *Dislocations in Crystals*, London: McGraw-Hill, 1953.

Stigh, U., A finite element study of threading dislocations, *Mech. Mater.*, vol. **14**(3), pp. 179–187, 1993.

Teodosiu, C., A dynamic theory of dislocations and its applications to the theory of the elastic plastic continuum, in Simmonds, A., Ed., *Fundamental Aspects of Dislocation Theory*, vol. **317**(2), pp. 837–876, *National Bureau of Standards Special Publication*, 1970.

Teodosiu, C., *Elastic Models of Crystal Defects*, Berlin and Bucureşti: Springer-Verlag and Editura Academiei, 1982.

Young, T. D., Kioseoglou, J., Dimitrakopulos, G. P., Dłużewski, P., and Komninou, P., 3D modelling of misfit networks in the interface region of heterostructures, *J. Phys. D: Appl. Phys.*, vol. **40**, pp. 4084–4091, 2007.

APPENDIX: SIMPLE SHEAR MODE

Consider a distortion tensor $\widehat{\boldsymbol{\beta}} = \widehat{\alpha}_{\circ}\widehat{x}\,\widehat{\mathbf{s}} \otimes \widehat{\mathbf{m}}$, where $\widehat{\alpha}_{\circ}$ is a constant, $\widehat{x}$ is one of the coordinates of an orthonormal system $\{\widehat{x}, \widehat{y}, \widehat{z}\}$, and $[\widehat{\mathbf{s}}] = [1,0,0]^T$ is a slip vector located on slip plane $[\widehat{\mathbf{m}}] = [0,1,0]^T$. The mentioned unit vectors rotate according to the well-known geometrical relations

$$\mathbf{m} = \frac{\mathbf{F}_{\mathrm{e}}^{-T}\widehat{\mathbf{m}}}{\left|\mathbf{F}_{\mathrm{e}}^{-T}\widehat{\mathbf{m}}\right|} \quad \text{and} \quad \mathbf{s} = \frac{\mathbf{F}_{\mathrm{e}}\widehat{\mathbf{s}}}{\left|\mathbf{F}_{\mathrm{e}}\widehat{\mathbf{s}}\right|}. \tag{40}$$

In our case $\mathbf{F}_{\mathrm{e}} = \begin{bmatrix} 1 & \widehat{\beta} & \cdot \\ \cdot & 1 & \cdot \\ \cdot & \cdot & 1 \end{bmatrix}$, which gives $\mathbf{m} = \widehat{\mathbf{m}}$ and $\mathbf{s} = \widehat{\mathbf{s}}$. In the linear theory, the differentiation of distortions over the current and reference positions are not distinguished and, according to relations (3) and (14), the additive decomposition of $\boldsymbol{\beta}(\mathbf{x}) = \beta(x)\,\mathbf{s} \otimes \mathbf{m}$ leads directly to the wanted relation $\boldsymbol{\alpha}_{\mathrm{e}} = 1/2\boldsymbol{\alpha} = \boldsymbol{\alpha}_{\mathrm{w}}$.